



INSTITUT DE FRANCE
Académie des sciences

Comptes Rendus

Chimie


Yingna Du, Liyuan Zhang, Rui Jing, Yongfei Li, Bo Yang and Gang Chen

Aquathermolysis of heavy oil catalyzed by transition metal salts and clay

Volume 26 (2023), p. 145-155

Published online: 13 September 2023

<https://doi.org/10.5802/crchim.237>

 This article is licensed under the
CREATIVE COMMONS ATTRIBUTION 4.0 INTERNATIONAL LICENSE.
<http://creativecommons.org/licenses/by/4.0/>



Les Comptes Rendus. Chimie sont membres du
Centre Mersenne pour l'édition scientifique ouverte
www.centre-mersenne.org
e-ISSN : 1878-1543



Research article

Aquathermolysis of heavy oil catalyzed by transition metal salts and clay

Yingna Du^{a, b}, Liyuan Zhang^{a, c}, Rui Jing^d, Yongfei Li^a, Bo Yang^{a, b}
and Gang Chen^{* a, b}

^a Shaanxi Province Key Laboratory of Environmental Pollution Control and Reservoir Protection Technology of Oilfields, Xi'an Shiyou University, Xi'an, 710065, China

^b Shaanxi University Engineering Research Center of Oil and Gas Field Chemistry, Xi'an Shiyou University, Xi'an, 710065, China

^c No.11 Oil Production Plant, PetroChina Changqing Oilfield Company, Xi'an, 710060, China

^d Xi'an Changqing Chemical Group Co., Ltd, PetroChina Changqing Oilfield Company, Xi'an, 7160065, China

E-mails: 1294138205@qq.com (Y. Du), zlyuan_cq@petrochina.com.cn (L. Zhang), 1156947308@qq.com (R. Jing), yfli@xsyu.edu.cn (Y. Li), youngbo1120@hotmail.com (B. Yang), gangchen@xsyu.edu.cn (G. Chen)

Abstract. Currently, researchers have indicated that inorganic minerals in reservoirs, such as clay minerals, carbonates and quartz, can catalyze the evolution of organic matter into oil and gas. Therefore it is reasonable to believe that the minerals in reservoirs may act as a catalyst support with the metal-containing catalyst added from outside during the thermal recovery of heavy oil. This paper studied the aquathermolysis of heavy oil catalyzed by minerals and transition metal. The reaction conditions of two heavy oil samples were investigated. The results show that the optimal reaction conditions of heavy oil from Xinjiang Baikouquan Oilfield (XBO) are the reaction temperature of 250 °C and the reaction time of 6 h; for the crude oil from Xinjiang Tahe Oilfield (XTO), the optimal reaction conditions are determined to be the reaction temperature of 250 °C and the reaction time of 12 h, the water-oil ratio of the two oils is 0.3. Under optimal conditions, viscosity and pour point of heavy oil are significantly reduced. Differential scanning calorimetry (DSC), GC-MS analysis, thermogravimetric analysis (TGA), and elemental analysis were used to study the properties of the two heavy oil samples before and after reaction to explore the mechanism of the catalyzed aquathermolysis of heavy oil. This work will benefit the related heavy oil recovery work in this field.

Keywords. Aquathermolysis, Viscosity reduction, Heavy oil, Transition metal, Clay, Catalysis.

Funding. This research was funded by National Science Foundation of China (50874092) and the Youth Innovation Team of Shaanxi University and Postgraduate Innovation Fund Project of Xi'an Shiyou University (YCS21211045).

Manuscript received 27 January 2023, revised 18 May 2023, accepted 20 June 2023.

* Corresponding author.

1. Introduction

The current heavy oil reserves are approximately 5.6 trillion barrels [1–4]. However, heavy oil has the characteristics of high density, high viscosity, poor fluidity and complex composition, which lead to difficulties in its extraction, transportation and subsequent processing [5,6]. Therefore, it is necessary to carry out research on the viscosity reduction technology of heavy oil, and it is necessary to solve the problems existing in the process of exploitation and transportation [7,8]. The initial method was to use superheated water or steam to heat heavy oil to reduce its viscosity and make it easier to flow, thereby enhancing heavy oil recovery [9,10]. There are the two main types of heavy oil viscosity reduction technologies: physical and chemical. The former is primarily based on the addition of crude oil flow improvers during the hot injection process, which is a simple and low-cost method. Gu [11] and Chen *et al.* [12,13] investigated and synthesized a variety of alkylbenzene sulfonates, some of which were able to achieve a viscosity reduction rate higher than 90%. When the alkylbenzene sulfonate co-crystallizes with the saturated hydrocarbon in crude oil, it causes disordering of the wax particles and results in a lower pour point. Nonionic surfactants were also studied as a means of improving the viscosity and pour point of crude oil [14]. In their research, Zhou *et al.* [15] utilized barium alkylbenzene sulfonate as the main synthetic material. It was shown that crude oil flow improvers can prevent the crystallization of saturated hydrocarbons in heavy oil and effectively reduce the viscosity of heavy oil. In addition, many researchers have explored polymers as potential viscosity reducing agents. Lv *et al.* [16], synthesized a functional copolymer viscosity reducer with mixed esters, 4-vinylpyridine and styrene monomers, indicating that the steric hindrance of copolymer viscosity reducer molecules destroys the interlocking structure of asphaltenes, which helps to reduce the viscosity of heavy oil. Zhang *et al.* [17] modified waste polystyrene with acetic anhydride, which can effectively reduce environmental pollution while also reducing heavy oil viscosity and improving crude oil fluidity. The purpose of chemical viscosity reduction technology is to reduce the viscosity of heavy oil by incorporating a catalyst into the aquathermolysis process. At present, there are four types

of catalysts; transition metal water-soluble catalysts, transition metal oil-soluble catalysts, acid–base catalysts, and ionic liquid catalysts [18]. In the process of steam injection, the addition of catalyst facilitates the pyrolysis of asphaltene and resin molecules into small molecular aquathermolysis products [19], thereby improving the viscosity and fluidity of heavy oil [20–22] and solving the problems of difficulty and high cost of heavy oil exploitation. Therefore, this method is widely used [23]. Many researchers have also done a lot of research work on heavy oil aquathermolysis and prepared a series of catalysts to conduct aquathermolysis viscosity reduction experiments on heavy oil from different oilfields in China, and the viscosity reduction rate can reach about 80% [24,25]. Chen *et al.* [26,27], investigated aquathermolysis of heavy oil at low temperature catalyzed by Zn (II) coordination complexes and Co (II) complexes, respectively. The reaction of catalyst and alcohol occurred at low temperature, which proved that the combination of catalyst and alcohol had a synergistic effect, which was helpful to greatly reduce the viscosity of heavy oil and improve its quality. Chen [28,29] conducted in-depth and meticulous research on the catalyzed reaction of aquathermolysis at the molecular level, deduced a large number of catalyzed mechanisms of the cracking reaction using kinetics, and proposed several new catalyzed reaction models. Ming *et al.* [30], developed an in situ synthesis strategy using well-dispersed CuO nanoparticles as an aquathermolysis catalyst to study the mechanism of viscosity reduction of heavy oil in the catalyzed system.

Although researchers have conducted extensive studies on catalyzed aquathermolysis of heavy oil, the effect of the indoor simulation experiment cannot be replicated in the oil field. This is because the indoor simulation experiment does not consider the effect of minerals in the oil reservoir on the addition of exogenous catalysts. On the other hand, in the traditional heavy oil viscosity reduction technology, inorganic salts and water are added to the heavy oil, but some metal cations will combine with OH^- in water to form hydroxide precipitates, resulting in poor viscosity reduction effect. The transition metal cation may adsorb on/in bentonite, which forms a new catalyst in the aquathermolysis. There are many kinds of minerals in the oil reservoir of oilfield. At present, studies have shown that inorganic minerals such as

clay minerals, carbonates, and quartz have catalytic effects on the transformation of organic matter into oil and gas. When the exogenous catalyst enters the oil reservoir, the oil reservoir minerals may adsorb or exchange ions to form a complex, which catalyzes the aquathermolysis reaction. A typical representative of clay reservoir minerals can adsorb metal cations by lattice substitution at the negatively charged surface. Therefore, we studied the aquathermolysis catalyzed by bentonite-supported transition metals to evaluate the influence of reservoir minerals on the external catalyst.

2. Materials and methods

2.1. Materials

The chlorides used in the experiment, such as ferrous chloride, ferric chloride, cobalt chloride, and copper chloride were purchased from National Group Chemical Reagent Co., Ltd. The liquid reagents are analytically pure reagents without further purification. The heavy oil used for evaluation is from Xinjiang Baikouquan Oilfield (XBO) and Xinjiang Tahe Oilfield (XTO), properties of which are shown in Table 1.

Each fraction (saturates, aromatics, resins and asphaltenes) content in the heavy oil sample was quantitatively analyzed based on the standard of SY/T 5119-2008 [31]. The pour point was measured according to SY/T 2541-2009 [32]. The viscosity of the crude oil sample was measured according to the standard of SY/T 0520-2008 [33].

2.2. Initial crude oil reaction, product separation and analysis

The water/oil mass ratio of the aquathermolysis of the two oil samples was selected according to the method described in [34]; the temperature and duration of the aquathermolysis were selected according to the method described in [35].

2.3. Preparation catalyst

Calcium bentonite and sodium bentonite were hydrated for 6 h. The transition metal chloride was

added to the hydrated bentonite in a 1.1 mass ratio (the bentonite:chloride molar ratio is 1:1.5). After stirring for 3 h, vacuum distillation, washing, drying, filtering and grinding the residue, the bentonite-supported transition metal ion catalyst was obtained. The names of the catalysts are shown in Table 2.

2.4. Catalyzed aquathermolysis reaction of heavy oil

Heavy oil and water were added successively with a mass ratio of 0.3 into the reactor. After catalyst addition, the reactants were heated to 180 °C and stirred. The mixture was cooled, and then the pour point and viscosity of the crude oil were evaluated [36].

2.5. Elemental analysis

The elemental compositions (C, H, N and S) of initial oil and treated oil were measured by an element analyzer in accordance with China Petroleum Industry Standard SY/T 5119-2016.

2.6. Thermogravimetric analysis

The TGA was conducted on a TGA/DSC 8220 (Mettler Toledo, Switzerland) instrument over a temperature range of 30–600 °C, under nitrogen atmosphere at a heating rate of 10 °C/min [37].

2.7. Differential scanning calorimetry (DSC) analysis

Differential scanning calorimetry (DSC) analysis of waxy crude oil samples was performed on a DSC822e DSC (Mettler Toledo, Switzerland) in a nitrogen atmosphere at a flow rate of 20 ml/min at a scan rate of –30 to 80 °C at 11 °C/min, and a cooling rate of 8 °C/min. The wax precipitation point of heavy oil was measured according to SY/T 0545-2012.

2.8. GC-MS analysis of saturated hydrocarbon components of heavy oil.

A HP-5 type capillary chromatographic column (0.32 mm × 30 m, 0.25 μm) was used. The temperature of the injection port was 300 °C, the temperature of the detector was 280 °C. The temperature

Table 1. Crude oil physical parameters

Crude oil	Pour point (°C)	Water content (%)	Saturated HC (%)	Aromatic HC (%)	Resin (%)	Asphaltene (%)
XBO	5.3	11.41	48.50	21.00	19.07	0.02
XTO	14.4	0.17	42.13	19.70	21.83	13.44

Table 2. List of catalysts

Metal chloride	Calcium bentonite	Sodium bentonite
Ferrous chloride	CB-1	NB-1
Ferric chloride	CB-2	NB-2
Cobalt chloride	CB-3	NB-3
Copper chloride	CB-4	NB-4

was programmed as follows: the starting temperature was 40 °C, held for 0.5 min; the temperature was increased to 120 °C at a rate of 5 °C/min, and then to 280 °C at 10 °C/min, and then maintained for 2.00 min.

3. Results and discussion

3.1. Characterizations of catalyst

It can be seen from Figure 1 that the metal-containing crystallites are tightly adsorbed on the scaly surface of bentonite and the inner wall of the pores, which increases the contact site of metal crystals with crude oil. The catalytic activity of a solid catalyst is directly proportional to its specific surface area. Therefore, by loading metals onto bentonite, its catalytic efficiency can be significantly improved.

3.2. The effect of catalyzing heavy oil aquathermolysis upgrading

Heavy oil was added to the reactor with a water/oil ratio of 0.3 and the catalysts were then screened with a 0.05% mass ratio to heavy oil under the optimized conditions mentioned above. During aquathermolysis of XBO, it can be seen in Figure 2(a,b) that the prepared catalysts did show some desired impact. The viscosity reduction effect of catalyst CB-4 was the best. Compared with the blank oil sample, the

viscosity of XBO was reduced by 37.1% (50 °C), and the viscosity of XBO was reduced by 21.5% (50 °C). However, the effect on XTO was obviously reflected in Figure 2(c,d) CB-1 can catalyze aquathermolysis of XTO effectively with a viscosity-reduction rate of 68.2% (50 °C) and NB-1 can catalyze the aquathermolysis of XTO effectively with a viscosity reduction rate of 66.2% (50 °C).

Comparison of the experiments above show that the aquathermolysis process of XBO and XTO catalyzed by this series of catalysts contains the cracking reaction and the polymerization reaction at the same time. The cause of the low reduction in viscosity is hypothesized to be either the complex reaction of metal ions with the heavy oil, which results in the formation of coke particles and lumps, or the free radical polymerization of the C-S intermediates produced by aquathermolysis, resulting in a significant amount of macromolecular substances. Nickel could affect the quality of crude oil [22] and pollute refining catalysts, so the bentonite-supported Ni (II) catalyst was not investigated further. Zn (II) has no activity and is not listed here.

3.3. Differential scanning calorimetry (DSC) analysis

Differential scanning calorimeter (DSC) analysis was conducted to study the wax formation process in untreated and treated XTO crude oil. CB-1 and NB-1 with relatively high catalytic activity for XTO were selected for DSC analysis of XTO before and after the catalyzed reaction. It can be seen from Figure 3 that the DSC curve of XTO shifts significantly to the left after the catalyzed aquathermolysis. The wax precipitation point decreased from 30.8 °C to 27.1 °C and then to 26.9 °C. This demonstrates that after the reaction, a portion of the heavy components in the oil sample are decomposed into lighter components, while the lighter components additionally dissolve a portion of the heavy components, slowing the precipitation of

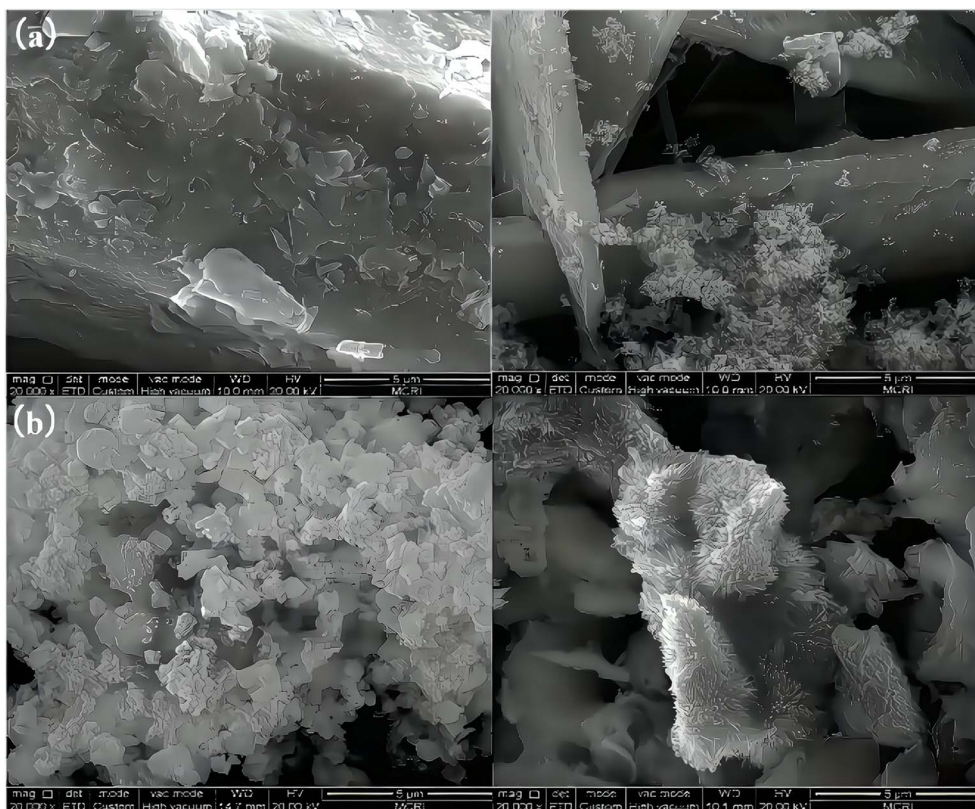


Figure 1. SEM images of calcium bentonite (left) and sodium bentonite (right) before and after loading (a) before loading; (b) after loading.

wax particles and lowering the oil sample's wax precipitation point.

3.4. Thermogravimetric analysis

CB-1 and NB-1 have a high catalytic effect on XTO as was seen during thermogravimetric analysis of XTO before and after the catalyzed reaction. Figure 4 (catalyst vs. oil sample) shows that the weight loss curve of XTO shifted to the left before and after the catalyzed aquathermolysis. The weight loss rates of XTO before and after adding the catalysts CB-1 and NB-1 to the aquathermolysis at 50–200 °C were 19.9%, 23.0%, and 22.5%, respectively, and the weight loss rates at 200–350 °C were 33.7%, 32.9%, and 32.9%, respectively, 32.5%, and the weight loss rates at 350–500 °C were 32.4%, 29.3% and 29.5%, respectively. As can be seen, the oil sample's low-temperature portion weight loss rate increased while its high-temperature part weight loss rate reduced

before and after the aquathermolysis. This shows that the catalyzed aquathermolysis cracks a part of the high-boiling, difficult-to-decompose macromolecular substances in the heavy oil into small molecular substances with low boiling points.

3.5. Elemental analysis

The change in element contents (C, H, N, and S) of XTO before and after aquathermolysis reaction was determined by elemental analysis. It can be seen from Table 3 that the total proportion of C and H elements in XTO increases before and after CB-1 catalyzed reaction, indicating that CB-1 has higher catalyzed activity. After the aquathermolysis of heavy oil in the presence of water, C, H and, N content increases while S content decreases and the C/H ratio decreases, indicating that water provides hydrogen for the heavy oil aquathermolysis reaction. The proportion of S element fell by 0.31% with

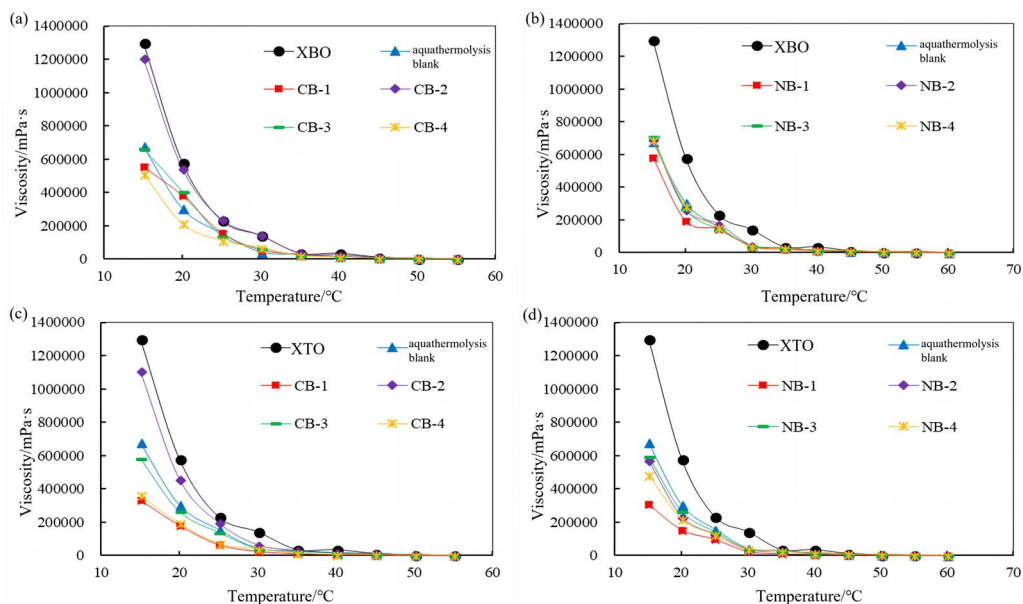


Figure 2. Viscosity effects of calcite and sodium clay supported catalysts for XBO treatment at different temperatures (a,b). Viscosity effects of calcite and sodium clay supported catalysts for XTO treatment at different temperatures (c,d).

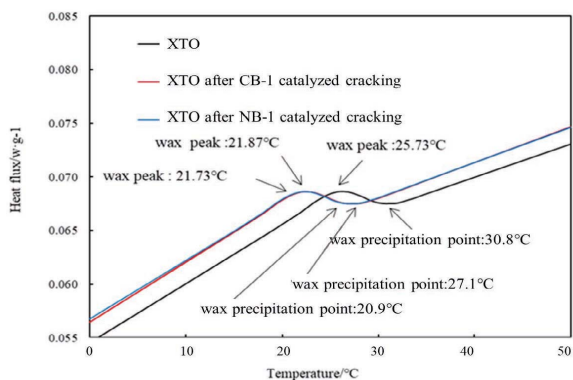


Figure 3. DSC curves of XTO before and after aquathermolysis.

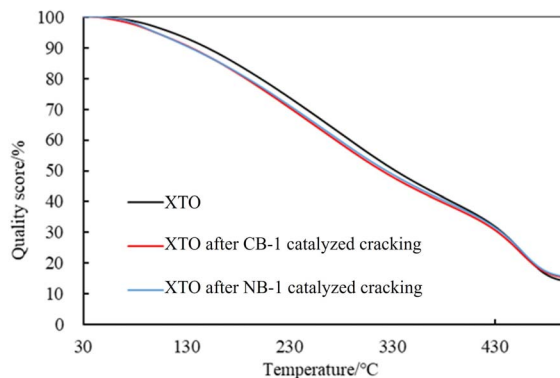


Figure 4. TGA curves of XTO oil samples under different reaction conditions.

aquathermolysis, by 0.38% with CB-1-catalyzed reaction. Since heteroatom-containing compounds are only found in colloid and asphaltene, the proportion of C and H elements in heavy oil increases after the reaction, while the proportion of S element decreases significantly, and the trend is essentially consistent with the viscosity reduction trend of heavy oil. This shows that the aquathermolysis process is

a series of reactions such as cracking, rearrangement, and hydrogenation of the C–S bonds of the sulfur-containing macromolecules in the resin asphaltene. Finally, the macromolecules are cracked into small molecules and the S element is converted into H₂S gas, reducing the S content in the oil sample.

Table 3. Element contents (C, H, N, and S) of XTO before and after the aquathermolysis reaction

	Name	C (%)	H (%)	N (%)	S (%)	C:H (%)
	Blank	79.12	11.21	1.70	2.45	7.06
XTO	CB-1	85.93	11.99	1.47	2.07	7.17
	CB-2	78.94	11.02	1.55	2.47	7.16
	CB-3	80.71	11.21	1.69	2.14	7.20
	CB-3	80.71	11.21	1.69	2.14	7.20

3.6. GC-MS analysis of saturated hydrocarbon components of heavy oil

The saturated hydrocarbon components were separated from XBO and XTO before and after the reaction by the national standard method, and the components were analyzed by GC-MS. The sample was made by dissolving 5% oil in chromatographically pure n-heptane, the peak detection limit was 2% of the maximum peak area, the solvent peak was excluded, and the maximum peak area matching compound is toluene. Figure 5 and Table 4 illustrate that the proportion of low-carbon components grew, the proportion of medium-carbon components increased and then reduced, and the proportion of high-carbon components increased and declined following the catalyzed reaction of XTO aquathermolysis. After adding CB-1, the components below C_{10} increased from 33.15% to 34.85%, the components between C_{10} – C_{15} increased from 44.29% to 47.00%, and the components between C_{15} – C_{20} decreased from 19.36% to 16.85%. The components above C_{20} are reduced from 3.20% to 1.20%. After adding NB-1, the components below C_{10} increased from 33.15% to 37.58%, the components between C_{10} – C_{15} decreased from 44.29% to 40.35%, the components between C_{15} – C_{20} increased from 19.36% to 20.50%, and the components above C_{20} are reduced from 3.20% to 1.57%.

The results show that the catalyst CB-1 has a higher cracking effect on the molecules of $>C_{15}$ in XTO, while the effect on the molecules of $<C_{15}$ is not obvious. The molecular catalysis effect of NB-1 on C_{10} – C_{15} in XTO is obvious but, in addition to catalyzing the cracking reaction, it also catalyzes the polymerization reaction, so that the proportion of C_{15} – C_{20} components increases after the reaction. The GC

Table 4. Carbon number distribution results of XTO before and after the reaction

Carbon number	XTO blank (%)	CB-1 (%)	NB-1 (%)
$<C_{10}$	33.15	34.85	37.58
C_{10} – C_{15}	44.29	47.00	40.35
C_{15} – C_{20}	19.36	16.85	20.50
$>C_{20}$	3.20	1.20	1.57

peaks of the oil samples were assigned by mass spectrometry in order to analyze the alterations of XTO before and after the reaction from the molecular structure. Table 5 lists some new molecules generated after the aquathermolysis.

The GC-MS results show that after reaction, the monocyclic and bicyclic compounds in n-alkanes and aromatic hydrocarbons increase, and a large amount of unsaturated hydrocarbons and heterocyclic aromatic hydrocarbons containing N, O elements is generated at the same time, which is due to the resin asphaltenes. The straight-chain hydrocarbon fragments resulting from ring-opening and side chain scission during aquathermolysis enter the saturated hydrocarbons while the cyclic cracking fragments enter the aromatic hydrocarbons.

3.7. Mechanism analysis

This catalyst includes metal ions and bentonite carriers. The loose pores and scaly structure of bentonite not only help to fix the catalyst center, but also help to disperse the crude oil, increase the surface area of the catalyst in contact with the resin and asphaltene molecules, boost the catalyst's selectivity and the efficiency of the aquathermolysis reaction. Metal ions promote the formation of free radicals by breaking the C–S bond, as shown in Figure 6. However, the viscosity of the oil sample decreases significantly after aquathermolysis catalyzed by calcium bentonite-supported catalyst, while it remains relatively unchanged after aquathermolysis catalyzed by sodium bentonite-supported catalyst. This may be due to the different pore sizes of the two kinds of bentonite, resulting in a greater difference in the degree of contact between water molecules and heavy oil. Water vapor in sodium bentonite cannot effectively spread to heavy oil, and there is insufficient active hydrogen

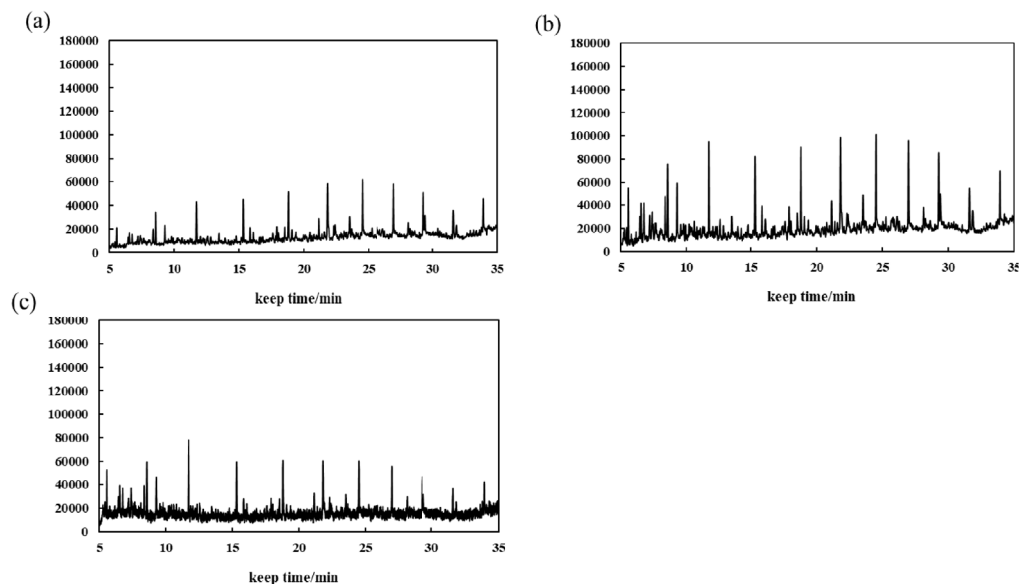
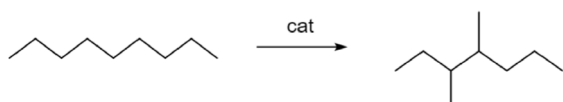


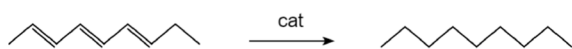
Figure 5. GC curves of XTO before and after the reaction (a) XTO, (b) CB-1-catalyzed aquathermolysis XTO, (c) NB-1-catalyzed aquathermolysis XTO.

to inhibit free radical polymerization. Therefore, the heavy oil coked severely after the reaction, which also increases the viscosity. According to the TGA curve analysis, some of the high boiling point and challenging to decompose macromolecular substances in heavy oil will be split into low boiling point small molecules during catalyzed aquathermolysis before and after the addition of exogenous catalyst. It is speculated from the structure of the compounds assigned by mass spectrometry that the following reactions may have occurred during the aquathermolysis catalysis process:

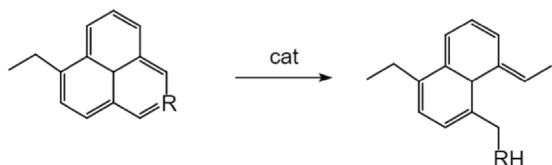
(1) Isomerization reaction



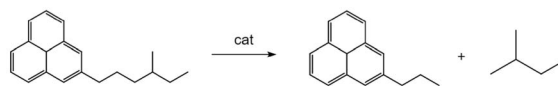
(2) Hydrogenation reaction



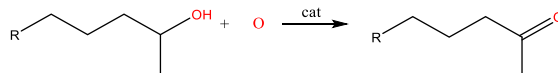
(3) Ring opening reaction



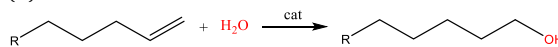
(4) Fragmentation reaction



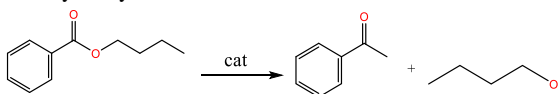
(5) Oxidation reaction



(6) Alcoholization reaction



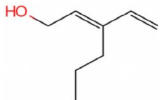
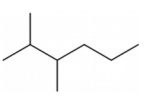
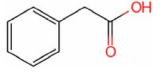
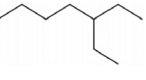
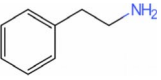
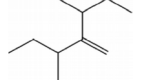
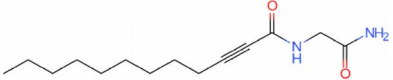
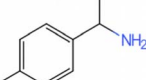
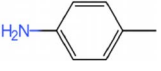
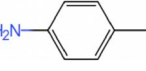
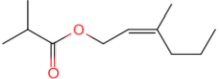
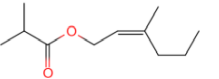
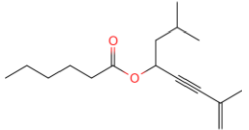
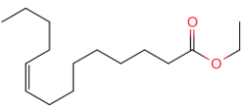
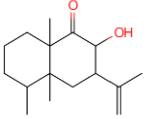
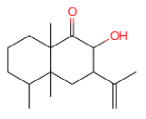
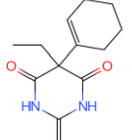
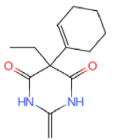
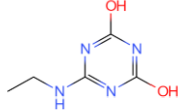
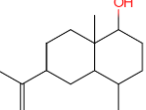
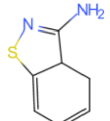
(7) Hydrolysis reaction of ester



4. Conclusions

In this work, a series of catalysts used in the aquathermolysis of heavy oil was prepared. The viscosity of the oil sample decreases after aquathermolysis catalyzed by calcium bentonite-supported catalyst, but not significantly after aquathermolysis catalyzed by sodium bentonite-supported catalyst. It has almost no catalytic activity on XBO but a high activity on XTO, reducing viscosity by 68.2%. This series of catalysts catalyzes the aquathermolysis to effectively break

Table 5. List of new molecules produced after the aquathermolysis reaction

Retention time (min)	Compound formula CB-1	Retention time (min)	Compound formula NB-1
5.277		4.649	
7.388		6.760	
7.454		4.013	
7.663		7.393	
10.281		10.281	
11.060		11.057	
11.907		14.790	
15.718		15.720	
17.607		17.609	
22.309		20.769	
24.524			

the C-S bond of resin and asphaltene molecules in the XTO and crack the macromolecules into small molecules of alkanes, olefins, and aromatic hydro-

carbons, lowering the viscosity and pour point of heavy oil. This work will benefit related work in this field.

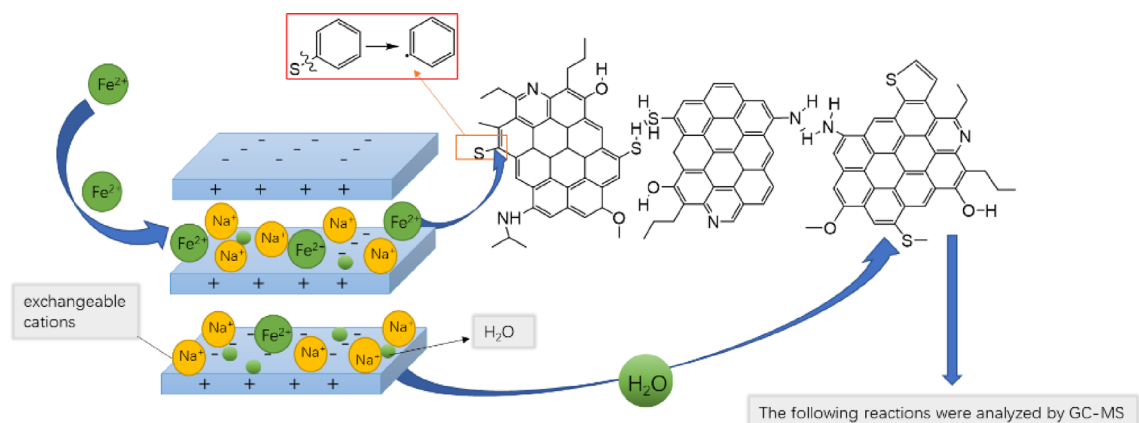


Figure 6. Catalytic mechanism of in situ and exogenous catalyst.

Conflicts of interest

The authors declare no conflicts of interest.

Acknowledgments

We thank the work of Modern Analysis and Testing Center of Xi'an Shiyou University.

References

- [1] N. Panariti, A. Del Bianco, G. Del Piero, *Appl. Catal. A: Gen.*, 2000, **204**, 215-222.
- [2] J. G. Speight, *Catal. Today*, 2004, **98**, 55-60.
- [3] H. Puron, P. Arcelus-Arrillaga, K. K. Chin *et al.*, *Fuel*, 2014, **117**, 408-414.
- [4] F. S. Alhumaidan, A. Hauser, M. S. Rana *et al.*, *Fuel*, 2015, **150**, 558-564.
- [5] H. Y. Li, K. X. Cui, L. Jin *et al.*, *J. Pet. Sci. Eng.*, 2018, **170**, 374-382.
- [6] R. Martínez-Palou, M. L. Mosqueira, B. Zapata-Rendón *et al.*, *J. Pet. Sci. Eng.*, 2011, **75**, 274-282.
- [7] L. Ma, R. Guo, S. Dong *et al.*, *Chem. Eng. J.*, 2023, **453**, article no. 139872.
- [8] Z. Wangyuan, L. Qi, L. Yongfei *et al.*, *Catalysts*, 2022, **12**, article no. 1383.
- [9] R. Guo, W. Fu, L. Qu *et al.*, *Processes*, 2022, **10**, article no. 1956.
- [10] Z. Zhichao, Z. Wangyuan, Y. Tao *et al.*, *Molecule*, 2023, **28**, article no. 2651.
- [11] W. Peng, G. Xuefan, X. Ming *et al.*, *J. Clean. Prod.*, 2022, **358**, article no. 131903.
- [12] G. Xuefan, G. Long, L. Yongfei *et al.*, *Pet. Chem.*, 2020, **60**, 140-145.
- [13] C. Gang, Z. Zhichao, S. Xiaodan *et al.*, *Fuel*, 2021, **288**, article no. 119644.
- [14] G. Xuefan, W. Peng, G. Zhen *et al.*, *J. Chem. Soc. Pak.*, 2020, **42**, 488-494.
- [15] Z. Zhichao, Z. Wangyuan, Z. Futian *et al.*, *C. R. Chim.*, 2021, **24**, 83-89.
- [16] X. Lv, W. Fan, Q. Wang *et al.*, *Energy Fuels*, 2019, **33**, 4053-4061.
- [17] Z. Wangyuan, S. Michal, Z. Jie *et al.*, *Polymers*, 2021, **13**, article no. 2505.
- [18] S. Shaban, S. Dessouky, A. Badawi *et al.*, *Energy Fuels*, 2014, **28**, 6545-6553.
- [19] C. Ovalles, C. Vallejos, T. Vasquez, *Pet. Sci. Technol.*, 2003, **21**, 255-274.
- [20] L. Fangfang, Y. Shenglai, Y. Xin, *Oilfield Chem.*, 2014, **31**, 75-78.
- [21] W. Shoubin, L. Yongjian, S. Yuwang, *J. Daqing Pet. Inst.*, 2004, **28**, 25-27.
- [22] L. Shiyi, P. Sen, Z. Rongjun *et al.*, *Pet. Chem.*, 2020, **60**, 998-1002.
- [23] M. Al-Ruqeishi, T. Mohiuddin, L. Al-Saadi, *Arab. J. Chem.*, 2019, **12**, 4084-4090.
- [24] Z. Zhichao, S. Michal, Z. Wangyuan *et al.*, *Fuel*, 2022, **307**, article no. 124871.
- [25] M. Liwa, Z. Shu, Z. Xiaolong *et al.*, *J. Chem. Technol. Biotechnol.*, 2022, **97**, 1128-1137.
- [26] C. Gang, Z. Wei, Y. Jiao *et al.*, *Pet. Chem.*, 2016, **16**, 183-186.
- [27] C. Gang, Z. Wei, N. Yang *et al.*, *Russ. J. Appl. Chem.*, 2015, **57**, 278-283.
- [28] C. Yong, C. Yanling, Z. Ming, *Geol. Sci. Technol. Inform.*, 2005, **24**, 75-79.
- [29] W. Chuan, C. Yanling, W. Yuanqing, *Oilfield Chem.*, 2009, **26**, 121-123.
- [30] C. Ming, L. Chen, L. Guo-Rui *et al.*, *Pet. Sci.*, 2019, **16**, 439-446, English Version.
- [31] SY/T 5119-2008, *Column Chromatographic Analysis Method of Rock Soluble Organic Matter and Crude Oil Group Components*, China National Petroleum Corporation, Beijing, 2008.
- [32] SY/T0541-2009, *Crude Solidification Point Determination*

- Method*, China National Petroleum Corporation, Beijing, 2009.
- [33] SY/T0520-2008, *Determination of Crude Oil Viscosity by Rotational Viscometer Equilibrium*, China National Petroleum Corporation, Beijing, 2008.
- [34] S. Wang, A. F. Li, *Pet. Sci. Technol.*, 2018, **36**, 739-743.
- [35] H. Xu, C. Pu, *Chem. Technol. Fuels Oils*, 2018, **53**, 913-921.
- [36] H. Mei, L. Qingbiao, L. Ping, *Chem. React. Eng. Technol.*, 2007, **23**, 183-187.
- [37] J. Q. Hu, J. H. Gan, J. P. Li *et al.*, *Fuel*, 2017, **188**, 66-172.